Dinamika Teknik Mesin 16(2) (2026) 174-185

Dinamika Teknik Mesin
Jurnal Keilmuan dan Terapan Teknik Mesin
http://dinamika.unram.ac.id/index.php/DTM/index

# Mechanical and morphological characteristics of abaca fiber-reinforced polymer composites with different laminate counts for potential bumper applications

**M. Martijanti*, A.G. Pessireron**
Department of Mechanical Engineering, Faculty of Manufacturing Technology, Universitas Jenderal Achmad Yani, Cimahi, West Java 40513, Indonesia. Mobile: 081321736202
*E-mail: martijanti@lecture.unjani.ac.id (corresponding author)

*ARTICLE INFO*

*Article History:*
*Received 16-08-2026*
*Accepted 17-09-2026*
*Available online 01-10-2026*

*Keywords:*
*Abaca fiber*
*Polymer composites*
*Porosity*
*Mechanical properties*
*Bumper*

*ABSTRACT*

*This study evaluates sheet-form abaca-fiber composites containing three, four, and five laminae in epoxy and polyester matrices. The composites were fabricated using hand lay-up and vacuum bagging and assessed for porosity, tensile behavior, area-normalized Charpy impact toughness, and fracture morphology. Five candidate specimens were measured for porosity in each laminate-count–matrix combination. The highest-porosity candidate was excluded using a predefined quality-screening criterion, and four specimens were mechanically tested. Two-way ANOVA showed significant effects of laminate count and matrix type on tensile strength, tensile strain, elastic modulus, and impact toughness ($p < 0.05$). Their interaction was significant for tensile strength ($p = 0.005$) and tensile strain ($p = 0.018$), but not for elastic modulus or impact toughness. The five-lamina epoxy group achieved 19.70 ± 1.57 MPa tensile strength, 8.88 ± 2.17 GPa elastic modulus, and 397.80 ± 26.34 kJ/m² impact toughness. SEM observations linked better performance to closer fiber–matrix contact, smaller voids, and fewer delamination paths. Porosity screening reduced group-mean porosity by up to 25.94%, indicating potential selection bias. These laboratory-scale results require component-level crashworthiness and durability validation.*

*Dinamika Teknik Mesin, Vol. 16, No. 2, October 2026,* ***p. ISSN: 2088-088X, e. ISSN:*** **2502-1729**

## 1. INTRODUCTION

Natural fiber-reinforced composites are promising lightweight and environmentally responsible materials because their reinforcements are renewable and biodegradable (Kamarudin et al., 2022; Maiti et al., 2022).

https://doi.org/10.29303/dtm.v16i2.1365

Abaca fiber (Musa textilis) is particularly attractive because of its favorable physical and mechanical properties for polymer reinforcement (Sinha et al., 2021; Valverde et al., 2022; Kurien et al., 2023).

Abaca plants can grow under diverse geographical conditions and their fibers can be processed by stem cutting, fiber extraction, and drying. This accessibility, together with their relatively low density and favorable mechanical properties, supports the use of abaca fibers in bio-based composite products.

Previous studies have shown that fiber volume fraction strongly affects the mechanical response of abaca composites. Research on bio-polyethylene, HDPE, and abaca–glass hybrid composites demonstrates that fiber content, stacking sequence, and interface quality govern composite stiffness and strength (Paglicawan et al., 2021; Seculi et al., 2022; Seculi et al., 2023a).

Fiber geometry and surface treatment influence stress transfer and internal-defect formation in natural-fiber composites. Recent studies on banana-fiber/epoxy and alkali-treated abaca fibers show that reinforcement condition strongly affects mechanical performance and interfacial behavior (Nguyen and Nguyen, 2021; Valášek et al., 2021).

Seculi et al. (2023a) reported increased tensile modulus and stiffness for abaca-reinforced Bio-PE and HDPE, while Kurien et al. (2023) emphasized the industrial potential of strong abaca fibers. Surface modification can further improve interfacial adhesion and composite mechanical properties (Harsanti et al., 2024). Collectively, these findings highlight the importance of fiber length, fiber fraction, and fiber–matrix interfacial quality.

Recent micromechanical studies demonstrate that tensile and flexural performance depends not only on abaca-fiber content but also on effective interfacial bonding (Seculi et al., 2022; Seculi et al., 2023b, 2023c). SEM is therefore required to relate mechanical behavior to voids, fiber pull-out, resin coverage, and delamination.

However, most recent abaca-composite studies have focused on fiber fraction, surface treatment, short-fiber thermoplastic systems, or abaca–glass hybridization. Limited information is available on sheet-form abaca laminates processed by hand lay-up and vacuum bagging, particularly studies that simultaneously compare epoxy and polyester matrices, vary the laminate count, quantify porosity, and connect SEM-observed defects with tensile and impact behavior. This lack of integrated evidence makes it difficult to determine whether adding laminae improves mechanical performance or merely increases void formation and delamination.

The novelty of this study is the integrated evaluation of three-, four-, and five-lamina sheet-form abaca composites in epoxy and polyester matrices by combining porosity, tensile strength, tensile strain, elastic modulus, impact toughness, and SEM fractography. Unlike studies that evaluate these responses separately, the present work interprets the mechanical results through the size, distribution, and location of voids and the quality of the fiber–matrix interface. This approach is used to identify the laminate configuration with the most suitable balance of stiffness, strength, and impact-energy absorption for further laboratory-scale development as a potential automotive bumper material.

## 2. RESEARCH METHODS

The materials were 0.5-mm-thick sheet-form abaca laminae, epoxy resin and hardener, polyester resin and catalyst, mold-release wax, and vacuum-bagging consumables. The cured panel thickness was maintained at 5 mm to approximate the thickness of commercially available automotive bumpers.

A balanced two-factor experimental design was used. The independent variables were laminate count (three, four, and five abaca laminae) and matrix type (epoxy and polyester). Five candidate specimens were measured for porosity in every laminate-count–matrix combination. The candidate with the highest porosity was excluded under a predefined fabrication-quality screening rule, and four specimens per combination were mechanically tested. The screening decision was based only on porosity and was made before considering mechanical results. All five porosity measurements are reported to make the exclusion transparent. Mechanical data are reported as mean ± standard deviation. Two-way analysis of variance (ANOVA) was performed at $\alpha = 0.05$ to evaluate the main effects of laminate count and matrix type and their interaction. Partial eta squared ($\eta p^2$) was calculated as an effect-size measure. Residual normality and variance homogeneity were assessed using the Shapiro–Wilk and Levene tests, respectively. Because the design was balanced, ANOVA results were retained but interpreted cautiously when residual normality was not satisfied.

The nominal reinforcement fraction was estimated geometrically from the ratio of total abaca-lamina thickness to cured panel thickness, $V_{f,nom} = (n \times tl/tc) \times 100\%$, where n is the laminate count, tl is the single-lamina thickness (0.5 mm), and tc is the panel thickness (5 mm). Accordingly, the three-, four-, and five-lamina composites had nominal fractions of 30%, 40%, and 50%, respectively. Because this thickness-based calculation does not include the measured fiber and matrix densities, the values are treated as nominal geometric reinforcement fractions rather than independently measured fiber volume fractions.

The epoxy resin and hardener were mixed at a 1:1 mass ratio. For each matrix system, mold-release wax was applied to the mold before the abaca laminae were arranged by hand lay-up. Matrix was distributed over every lamina with a roller or brush to promote impregnation and minimize entrapped air.

The lay-up was enclosed in a vacuum bag and connected to a Single Stage Vacuum Pump VP115 with a nominal flow capacity of 1.5 CFM, an ultimate pressure of 5 Pa, and a power rating of 1/4 HP. Vacuum consolidation was maintained during room-temperature curing.

Polyester panels were cured for 12 h, whereas epoxy panels were cured for 24 h. The cured panels were demolded, finished to a uniform thickness of 5 mm, and machined to the specimen geometries required by the corresponding test standards.

Tensile testing was performed using an Instron 5982 universal testing machine in accordance with ASTM D638. Charpy impact testing was conducted using a WOLPERT PW 30/15 pendulum impact tester in accordance with ASTM D6110. The instrument provided the absorbed impact energy and final pendulum angle. Impact toughness was calculated manually from the absorbed energy and nominal fractured cross-sectional area beneath the notch using Equation (1), while the fracture area was calculated using Equation (2).

$$H_I = \frac{E_{abs}}{A_f} \tag{1}$$

$$A_f = bh_n \tag{2}$$

where HI is the impact toughness (J/m²), Eabs is the absorbed impact energy (J), Af is the nominal fractured cross-sectional area beneath the notch (m²), b is the specimen width (m), and hn is the remaining ligament thickness beneath the notch (m). Values obtained in J/m² were divided by 1000 and reported as kJ/m².

The mechanical results were evaluated comparatively among the fabricated laminate configurations. No full-scale bumper crash test was performed; therefore, the automotive interpretation is limited to identifying a promising material configuration for subsequent component-level validation.

## 3. RESULTS AND DISCUSSION

The experimental results are discussed in terms of porosity, tensile response, impact toughness, and the fiber–matrix morphology observed by SEM. The effects of laminate count and matrix distribution are considered together because voids and interfacial defects directly affect load transfer. Because the highest-porosity candidate in each set was excluded before mechanical testing, the reported tensile and impact results represent specimens that passed the porosity-based screening stage and should not be interpreted as random-sample averages of the entire fabricated population.

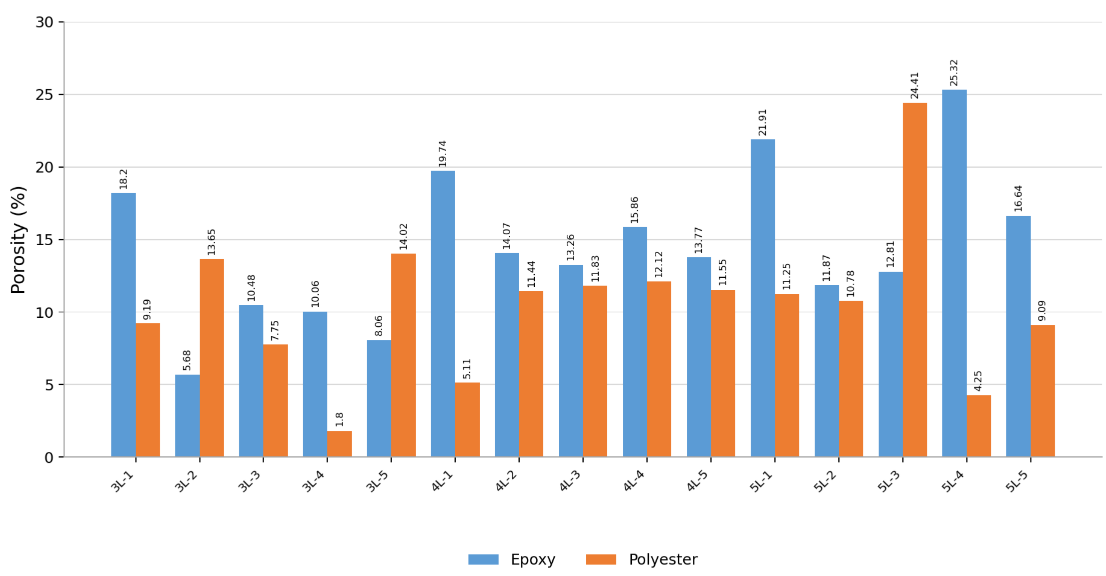


Figure 1. Porosity of the tensile-test specimens.

Figure 1 presents the porosity of all five tensile-candidate specimens for each laminate-count–matrix combination before screening. Across the complete dataset, the highest value was 25.32% for epoxy 5L-4, whereas the lowest was 1.80% for polyester 3L-4. The corrected polyester 4L-5 value is 11.55%. Within each laminate-count–matrix set, the single candidate with the highest porosity was excluded and the four lower-porosity specimens proceeded to tensile testing. The variation among replicates indicates that increasing laminate count can increase air entrapment when resin distribution and compaction are not uniform. This interpretation agrees with Jahanzeb et al. (2022), who related greater fiber packing to restricted resin flow and void formation. Vacuum bagging reduced bulk entrapped air but did not eliminate local incomplete wetting between adjacent abaca laminae.

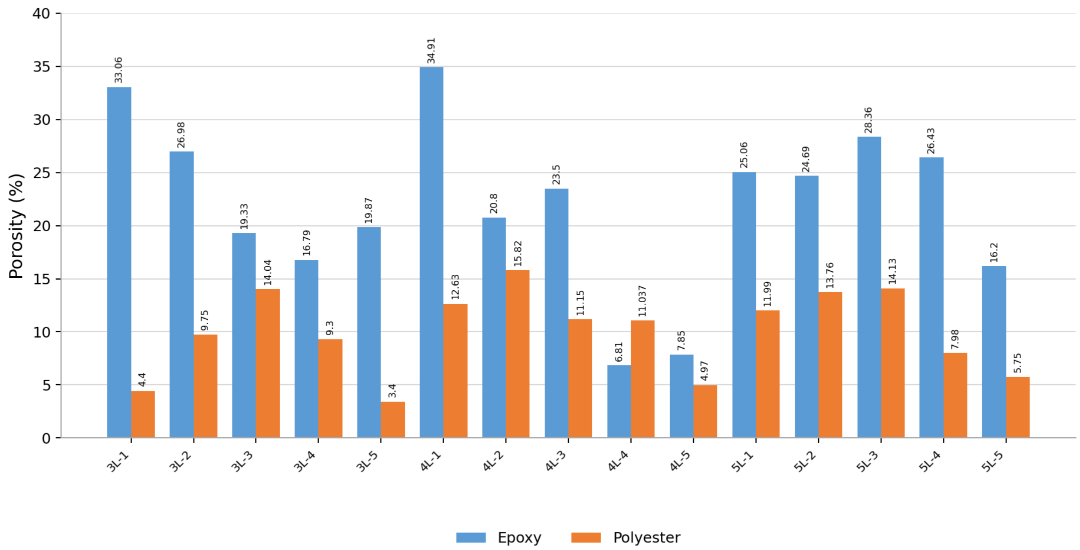


Figure 2. Porosity of the impact-test specimens.

Figure 2 presents the corresponding porosity screening for all impact-candidate specimens. Jahanzeb et al. (2022) explained that increasing fiber content may increase void formation because narrow spaces between fibers restrict resin flow. Imperfect fiber arrangement and incomplete impregnation consequently reduce fiber–matrix interfacial quality.

Across all impact candidates in Figure 2, the highest porosity was 34.91% for epoxy 4L-1 and the lowest was 3.40% for polyester 3L-5. The corrected epoxy 4L-5 value is 7.85%. The highest-porosity candidate in each laminate-count–matrix set was excluded before impact testing. The wide epoxy–polyester and replicate-to-replicate variation confirms that total porosity depends on impregnation and local consolidation, not solely on laminate count. The mechanical results below further show that defect size and position at load-bearing interfaces must be considered together with the total porosity percentage.

The tensile-strength results for the three laminate configurations are presented in Figure 3. For the epoxy matrix, the five-lamina group exhibited the highest mean tensile strength (19.70 ± 1.57 MPa), followed by 3L (16.43 ± 1.11 MPa), whereas 4L gave the lowest mean (8.38 ± 0.34 MPa). The corresponding polyester means were 18.60 ± 4.85, 16.63 ± 2.19, and 16.02 ± 2.07 MPa for 5L, 3L, and 4L, respectively. Thus, the previously reported values of 19.70, 16.53, and 8.38 MPa describe the epoxy trend and should not be interpreted as matrix-combined averages.

The low strength of the 4L configuration was attributed to delamination and locally weak interfaces. Delamination separates adjacent laminae and interrupts stress transfer, so an increase in laminate count does not automatically increase strength when consolidation quality is poor.

Recent abaca-composite interface studies similarly show that a strong interface enables the matrix to transfer tensile load to the fibers. Weak adhesion, fiber pull-out, and large voids concentrate stress and cause premature failure (Seculi et al., 2022; Seculi et al., 2023b).

The five-lamina group produced the highest average tensile strength among the tested configurations. This result identifies 5L as the strongest laboratory-scale configuration in the present dataset; it does not by itself establish compliance with a vehicle-bumper standard.

https://doi.org/10.29303/dtm.v16i2.1365

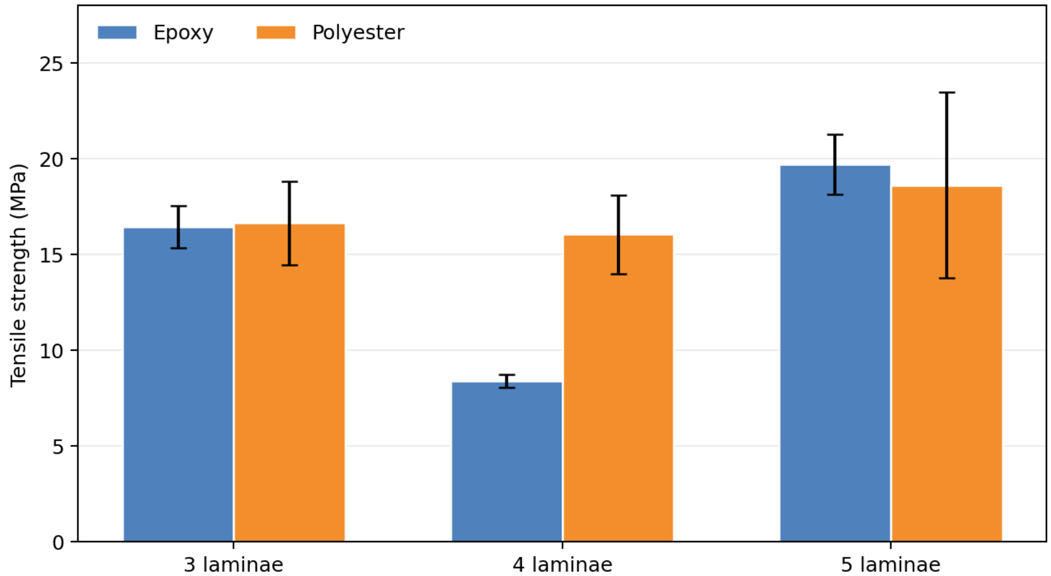


Figure 3. Mean tensile strength with standard-deviation error bars (n = 4).

The tensile-strain results for each laminate configuration are shown in Figure 4. For epoxy composites, mean tensile strain was 4.33 ± 0.47% for 3L, 5.33 ± 0.47% for 4L, and 2.33 ± 0.47% for 5L. Polyester composites showed 3.00 ± 0.82%, 3.33 ± 0.94%, and 2.33 ± 0.47%, respectively. Thus, the five-lamina groups had the lowest mean tensile strain for both matrices, indicating more restricted deformation at the highest nominal reinforcement fraction.

Two-way ANOVA showed significant effects of laminate count ($p < 0.001$), matrix type ($p < 0.001$), and their interaction ($p = 0.018$) on tensile strain. Because residual normality was not satisfied, these results are interpreted cautiously. The lower strain of the 5L groups indicates reduced ductility; therefore, laminate count should be evaluated together with strength and impact toughness rather than independently (Patel et al., 2023).

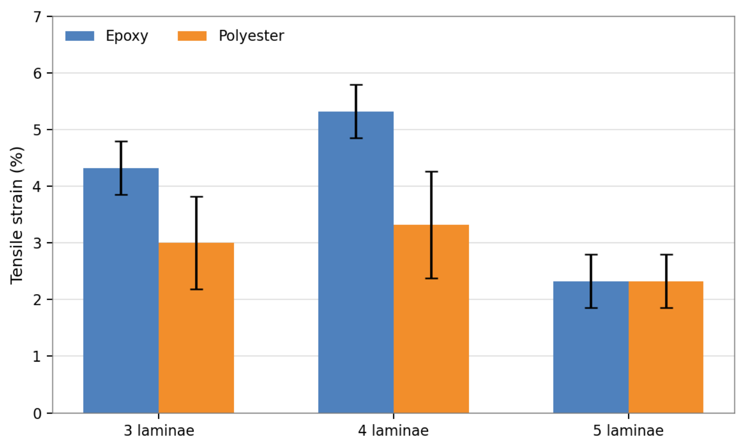


Figure 4. Mean tensile strain with standard-deviation error bars (n = 4).

The elastic-modulus results are presented in Figure 5. For epoxy composites, mean elastic modulus was 3.88 ± 0.41 GPa for 3L, 1.60 ± 0.08 GPa for 4L, and 8.88 ± 2.17 GPa for 5L. Polyester composites showed 6.23 ± 2.46, 5.50 ± 2.38, and 8.50 ± 3.24 GPa, respectively. The 5L configuration therefore provided the highest mean stiffness for both matrices, although replicate variability was appreciable, particularly for polyester.

The decrease for 4L again indicates that laminate architecture alone did not control stiffness. Delamination, voids, and uneven resin distribution reduced the effective load-bearing cross-section.

https://doi.org/10.29303/dtm.v16i2.1365

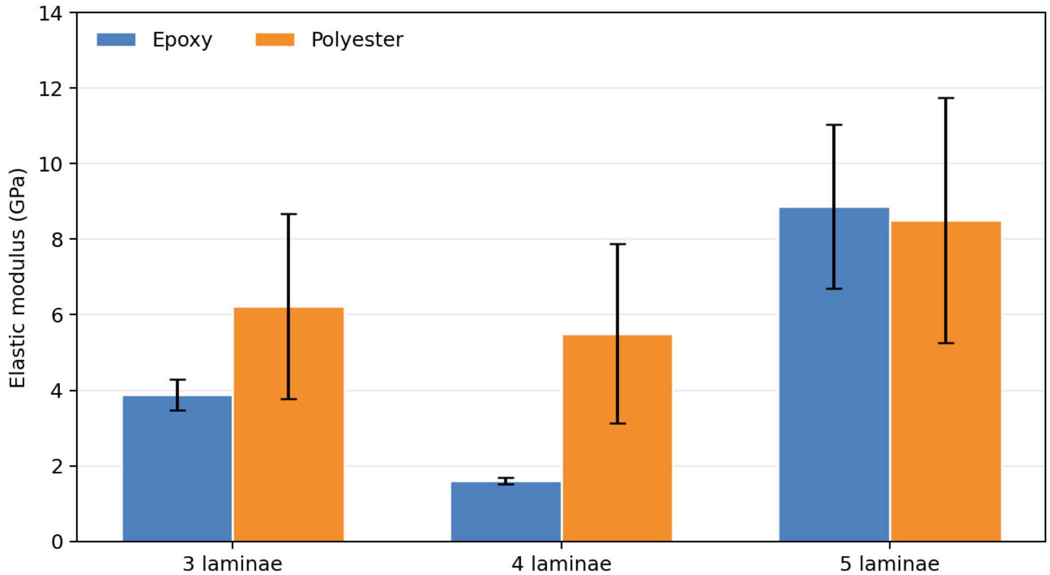


Figure 5. Mean elastic modulus with standard-deviation error bars (n = 4).

The impact-toughness results are presented in Figure 6. For epoxy composites, mean impact toughness was 351.00 ± 16.13 kJ/m² for 3L, 351.23 ± 21.78 kJ/m² for 4L, and 397.80 ± 26.34 kJ/m² for 5L. The corrected 4L mean is 351.23 kJ/m², not 353.75 kJ/m². Polyester means were higher at 407.30 ± 14.53, 435.33 ± 11.30, and 443.42 ± 30.27 kJ/m² for 3L, 4L, and 5L, respectively. Additional well-bonded laminae can provide interfaces for crack deflection, fiber bridging, and frictional energy dissipation.

Fiber fraction, orientation, and hybridization can significantly influence impact and wear behavior in abaca composites (Prakash et al., 2023; Vadivel and Venkatesh, 2025). Nevertheless, the benefit of additional reinforcement depends on uniform wetting; poorly bonded interfaces can initiate delamination instead of absorbing impact energy.

Two-way ANOVA showed significant effects of laminate count and matrix type on impact toughness ($p = 0.003$ and $p < 0.001$, respectively), while their interaction was not significant ($p = 0.200$). Polyester groups generally showed higher mean impact toughness than the corresponding epoxy groups. These results indicate independent contributions of laminate count and matrix type within the laboratory conditions evaluated.

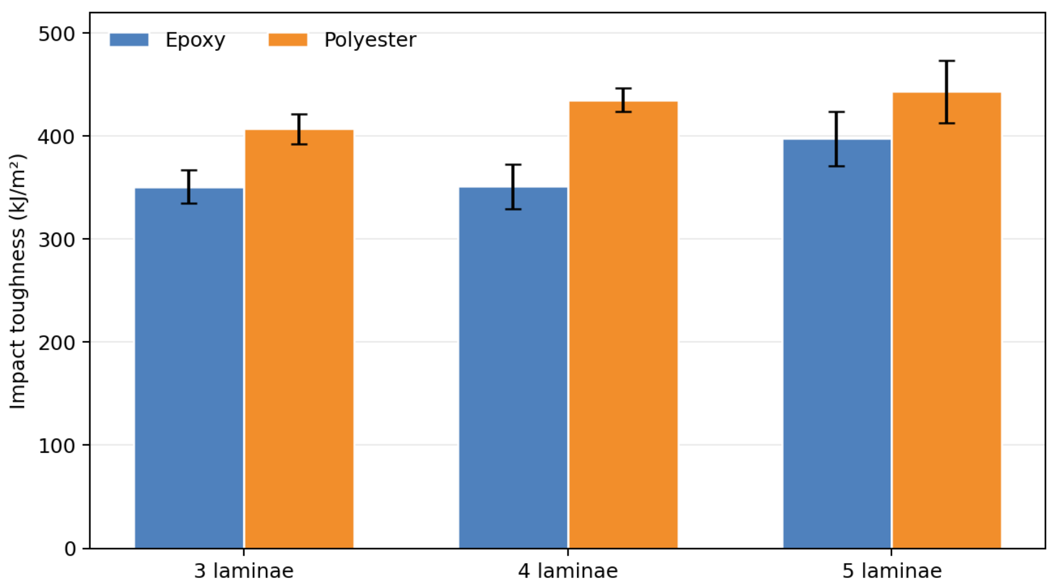


Figure 6. Mean impact toughness with standard-deviation error bars (n = 4).

https://doi.org/10.29303/dtm.v16i2.1365

The reported impact results identify the five-lamina configuration as the best energy-absorbing design among the specimens tested. Component-level impact, environmental durability, and crashworthiness tests are still required before the material can be qualified for a bumper application.

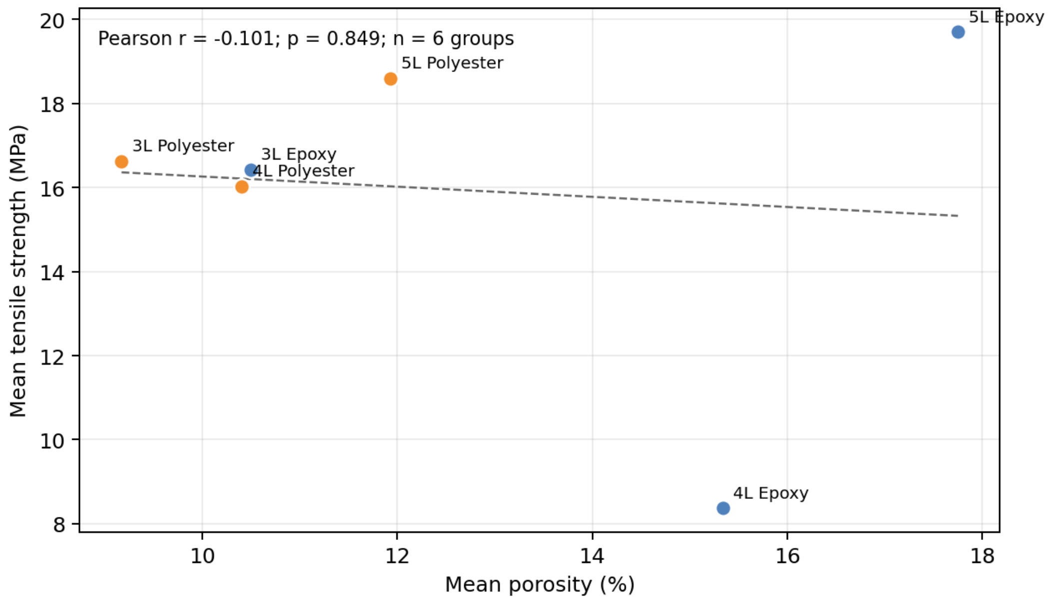


Figure 7. Mean tensile strength versus mean porosity.

Two-way ANOVA confirmed significant effects of laminate count and matrix type on all four mechanical responses. The interaction was significant for tensile strength and tensile strain, but not for elastic modulus or impact toughness (Table 1). Levene's tests supported homogeneity of variance for all responses ($p > 0.05$). Shapiro–Wilk tests indicated non-normal residuals for tensile strength, tensile strain, and elastic modulus. Those ANOVA results are therefore interpreted cautiously, although the balanced factorial design is relatively robust to moderate departures from normality.

Table 1. Two-way ANOVA results for the mechanical properties (n = 4 specimens per laminate-count–matrix combination).

| Response | Effect | df | F | p-value | Partial η² | Decision |
|---|---|---|---|---|---|---|
| Tensile strength | Laminate count | 2 | 16.210 | <0.001 | 0.643 | Significant |
| | Matrix type | 1 | 4.997 | 0.038 | 0.217 | Significant |
| | Laminate count × matrix type | 2 | 7.335 | 0.005 | 0.449 | Significant |
| Tensile strain | Laminate count | 2 | 20.370 | <0.001 | 0.694 | Significant |
| | Matrix type | 1 | 18.081 | <0.001 | 0.501 | Significant |
| | Laminate count × matrix type | 2 | 5.079 | 0.018 | 0.361 | Significant |
| Elastic modulus | Laminate count | 2 | 12.346 | <0.001 | 0.578 | Significant |
| | Matrix type | 1 | 5.088 | 0.037 | 0.220 | Significant |
| | Laminate count × matrix type | 2 | 2.071 | 0.155 | 0.187 | Not significant |
| Impact toughness | Laminate count | 2 | 7.949 | 0.003 | 0.469 | Significant |
| | Matrix type | 1 | 51.588 | <0.001 | 0.741 | Significant |
| | Laminate count × matrix type | 2 | 1.764 | 0.200 | 0.164 | Not significant |

Model $R^2$ values were 0.743 for tensile strength, 0.793 for tensile strain, 0.653 for elastic modulus, and 0.798 for impact toughness.

The sensitivity analysis showed that excluding the candidate with the highest porosity reduced the group-mean porosity by 4.09–25.94% in the tensile-specimen dataset and by 4.58–21.51% in the impact-specimen dataset. Therefore, the screening procedure altered the analyzed population and may have introduced selection bias. The mechanical results represent specimens that passed the porosity-based quality-screening criterion and should not be interpreted as unconditional averages of the manufacturing process.

Figure 7. Exploratory relationship between group-mean porosity and tensile strength (n = 6 groups). Because the mechanical-test identifiers could not be mapped unambiguously to the retained porosity-candidate identifiers after screening, an individual-specimen correlation was not calculated. Figure 7 therefore presents an exploratory comparison using the six laminate-count–matrix group means. The Pearson correlation between mean porosity and mean tensile strength was weak and not significant ($r = -0.101$, $p = 0.849$; $R^2 = 0.010$).

The group-level result indicates that total porosity percentage alone did not explain the tensile-strength differences among the tested groups. Void location, connectivity, resin-starved regions, and interfacial adhesion are likely to be more influential than a single bulk porosity value.

This analysis is exploratory because it uses only six group means and must not be presented as an individual-specimen correlation. A future study should preserve a single specimen identifier across porosity measurement, mechanical testing, and SEM characterization.

The relationship between impact toughness and porosity is shown in Figure 8. Figure 8 uses the six group means because specimen-level pairing could not be verified. Mean impact-candidate porosity showed a moderately strong negative association with mean impact toughness, but the relationship was not statistically significant (Pearson $r = -0.698$, $p = 0.123$; $R^2 = 0.487$). The result suggests a possible trend that requires confirmation with traceable specimen-level data and a larger sample size.

Delamination occurs when interlaminar stresses exceed local interface strength, while voids redirect stress toward weak regions. Consequently, void morphology, stacking quality, and interlaminar adhesion should be evaluated together rather than relying only on total porosity percentage.

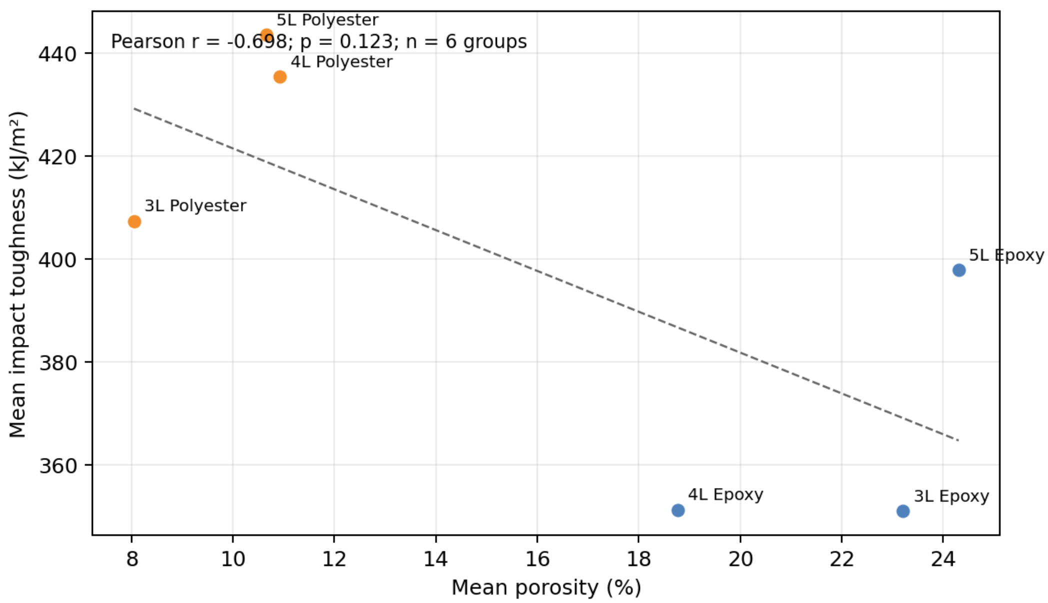


Figure 8. Exploratory relationship between group-mean porosity and impact toughness (n = 6 groups).

Figures 9 and 10 compare epoxy tensile specimens at 500× magnification. The 5L-3 specimen in Figure 9 shows comparatively continuous contact between the abaca laminae and epoxy matrix, with only small, dispersed voids. The larger bonded area enables shear stress to be transferred from the matrix to the reinforcement and restricts premature fiber pull-out. This morphology is consistent with the five-lamina epoxy group having the highest mean tensile strength (19.70 ± 1.57 MPa) and elastic modulus (8.88 ± 2.17 GPa), and it agrees with the interface-strength mechanism reported by Seculi et al. (2022, 2023b).

In contrast, the 4L-2 specimen in Figure 10 contains larger voids, resin-starved regions, and discontinuous fiber–matrix contact. These defects reduce the effective load-bearing area, concentrate stress at void edges, and provide paths for delamination. The observed morphology is consistent with the four-lamina epoxy group producing the lowest mean tensile strength (8.38 ± 0.34 MPa) and modulus (1.60 ± 0.08 GPa), despite containing more reinforcement than the three-lamina group.

https://doi.org/10.29303/dtm.v16i2.1365

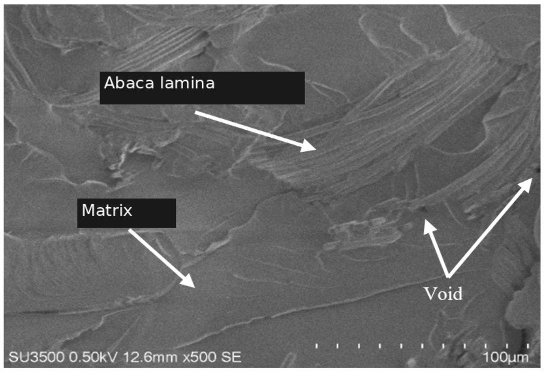


Figure 9. SEM micrograph of the epoxy tensile specimen with the highest strength.

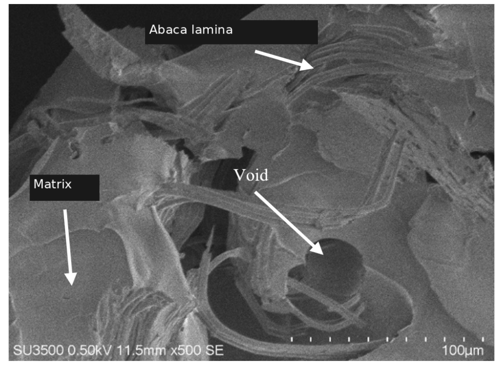


Figure 10. SEM micrograph of the epoxy tensile specimen with the lowest strength.

Figures 11 and 12 compare polyester tensile specimens at 500× magnification. The higher-strength polyester specimen in Figure 11 contains fewer and smaller voids and shows closer interfacial contact than the lower-strength specimen in Figure 12. Conversely, the large cavities and interfacial gaps in Figure 12 reduce the effective load-transfer area and initiate cracks under tensile loading. The comparison confirms that void morphology and interface continuity, rather than porosity percentage alone, control tensile failure, consistent with the micromechanical analyses of Seculi et al. (2022, 2023b).

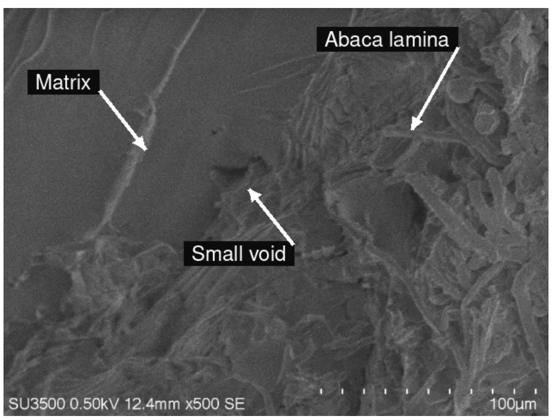


Figure 11. SEM micrograph of the polyester tensile specimen with the highest strength, showing close matrix–abaca contact, a relatively compact lamina region, and a small void.

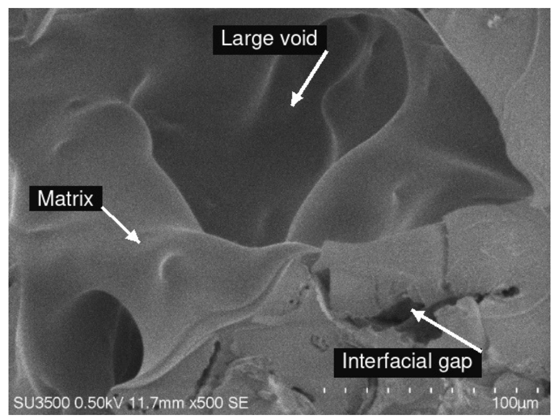


Figure 12. SEM micrograph of the polyester tensile specimen with the lowest strength, showing a large void and an interfacial gap in the surrounding matrix.

Figures 13 and 14 compare epoxy impact specimens at 500× magnification. The 5L-2 epoxy specimen exhibits relatively close fiber–matrix contact and numerous small voids. During impact, bonded laminae can deflect cracks, bridge the fracture path, and dissipate energy through controlled interfacial debonding and fiber pull-out. This morphology is consistent with the five-lamina epoxy group recording a mean impact toughness of 397.80 ± 26.34 kJ/m².

The representative lower-toughness epoxy specimen in Figure 14 contains larger voids and weaker interfacial contact. Large voids act as pre-existing cracks, while poorly bonded interfaces permit rapid delamination with limited frictional energy absorption. This morphology is consistent with the lower mean impact toughness of the three-lamina epoxy group (351.00 ± 16.13 kJ/m²) and reinforces the need to interpret impact performance together with defect geometry.

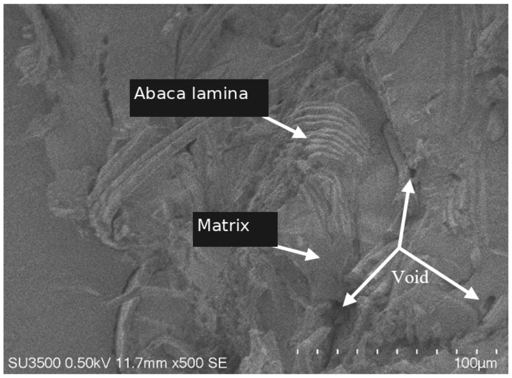


Figure 13. SEM micrograph of the epoxy impact specimen with the highest toughness.

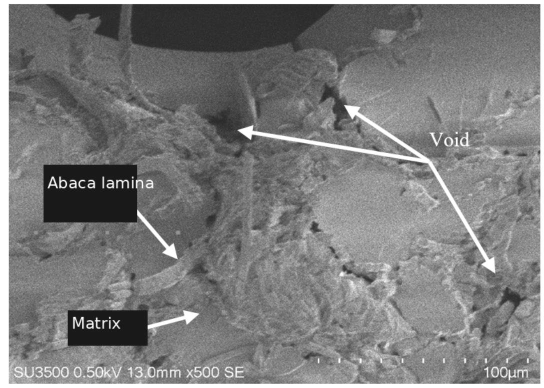


Figure 14. SEM micrograph of a representative lower-toughness epoxy impact specimen.

.

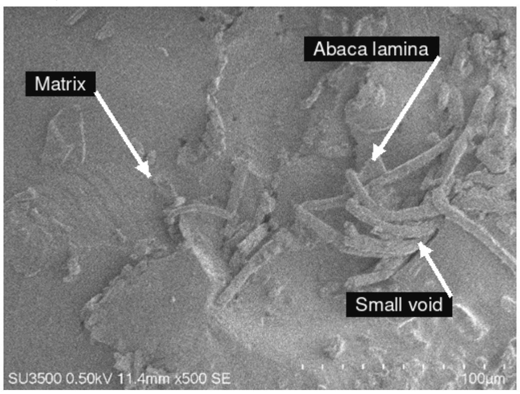


Figure 15. SEM micrograph of the polyester impact specimen with the highest toughness, showing a compact matrix–abaca region and a comparatively small void.

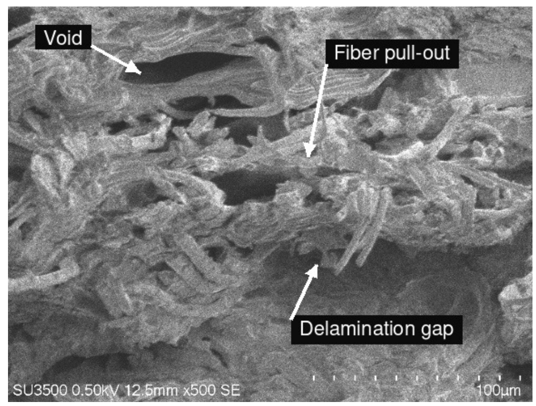


Figure 16. SEM micrograph of the polyester impact specimen with the lowest toughness, showing a void, fiber pull-out, and a delamination gap.

Figures 15 and 16 compare polyester impact specimens at 500× magnification. Figure 15 shows fewer and smaller voids and a denser polyester–abaca interface than Figure 16. The denser interface promotes crack deflection and frictional pull-out, whereas the large interconnected gaps in Figure 16 weaken interlaminar bonding and allow a crack to cross the section more directly. The SEM comparison therefore provides a physical explanation for the impact-toughness differences: compact interfaces absorb more energy, while large connected voids and delamination paths reduce the energy required for fracture. Similar dependence on reinforcement architecture and interface quality has been reported for abaca-based composites (Paglicawan et al., 2021; Seculi et al., 2023c).

The mechanical-property averages were calculated after porosity-based screening. The sensitivity analysis demonstrated measurable reductions in the group-mean porosity; therefore, selection bias cannot be excluded. The experimental design was limited to four mechanically tested specimens per laminate-count–matrix combination. Full-scale bumper crash tests, environmental ageing tests, fatigue tests, and long-term durability assessments were not conducted.

## 4. CONCLUSION

The experimental results support the following conclusions:

1. Porosity-based screening reduced group-mean porosity by 4.09–25.94% for tensile candidates and 4.58–21.51% for impact candidates. The mechanical findings therefore describe screened specimens, and selection bias cannot be excluded.

2. Laminate count and matrix type significantly affected tensile strength, tensile strain, elastic modulus, and impact toughness. Their interaction was significant for tensile strength and tensile strain, but not for elastic modulus or impact toughness.
3. The five-lamina groups provided the most favorable laboratory-scale response: the epoxy group reached 19.70 ± 1.57 MPa tensile strength and 8.88 ± 2.17 GPa modulus, while the polyester group reached 443.42 ± 30.27 kJ/m² impact toughness. SEM observations linked better performance to closer fiber–matrix contact and fewer critical defects.
4. These results support continued material development only. Automotive-bumper suitability still requires component-level impact, crashworthiness, fatigue, and environmental-durability testing.

## ACKNOWLEDGMENTS

The author gratefully acknowledges the Institute for Research and Community Service (LPPM), Universitas Jenderal Achmad Yani, for research funding. The author also thanks the Mechanical Engineering Study Program, Universitas Jenderal Achmad Yani, for providing laboratory facilities and technical support.

## REFERENCES

Harsanti, D., Novriadi, D., Pratama, A., Surface modification of abaca fibers with glutaraldehyde for improved mechanical properties of injection molded PLA biocomposites, Journal of Fibers and Polymer Composites, 3(1), 20–32, 2024. https://doi.org/10.55043/jfpc.v3i1.129.

Jahanzeb, S., Siddique, S.H., Hussain, D., Porosity and fiber orientation of banana fiber nonwoven webs using image analysis technique, Journal of Natural Fibers, 19, 6056–6073, 2022. https://doi.org/10.1080/15440478.2021.1904478.

Kamarudin, S.H., Mohd Basri, M.S., Rayung, M., Abu, F., Ahmad, S., Norizan, M.N., Osman, S., Sarifuddin, N., Mat Desa, M.S.Z., Abdullah, U.H., Amin Tawakkal, I.S.M., Abdullah, L.C., A review on natural fiber reinforced polymer composites (NFRPC) for sustainable industrial applications, Polymers, 14(17), 3698, 2022. https://doi.org/10.3390/polym14173698.

Kurien, R.A., Selvaraj, D.P., Sekar, M., Koshy, C.P., Paul, C., Palanisamy, S., Santulli, C., Kumar, P., A comprehensive review on the mechanical, physical, and thermal properties of abaca fibre for their introduction into structural polymer composites, Cellulose, 30(14), 8643–8664, 2023. https://doi.org/10.1007/s10570-023-05441-z.

Maiti, S., Islam, M.R., Uddin, M.A., Afroj, A., Eichhorn, S.J., Karim, N., Sustainable fiber-reinforced composites: A review, Advanced Sustainable Systems, 6(11), 2200258, 2022. https://doi.org/10.1002/adsu.202200258.

Nguyen, T.A., Nguyen, T.H., Banana fiber-reinforced epoxy composites: Mechanical properties and fire retardancy, International Journal of Chemical Engineering, 2021, 1973644, 2021. https://doi.org/10.1155/2021/1973644.

Paglicawan, M.A., Emolaga, C.S., Sudayon, J.M.B., Tria, K.B., Mechanical properties of abaca–glass fiber composites fabricated by vacuum-assisted resin transfer method, Polymers, 13(16), 2719, 2021. https://doi.org/10.3390/polym13162719.

Patel, R.V., Yadav, A., Winczek, J., Physical, mechanical, and thermal properties of natural fiber-reinforced epoxy composites for construction and automotive applications, Applied Sciences, 13(8), 5126, 2023. https://doi.org/10.3390/app13085126.

Prakash, V., Pradhan, S., Majhi, S., Acharya, S.K., Evaluation of dry sliding wear behavior of abaca/glass fiber hybrid composite for tribological applications, Proceedings of the Institution of Mechanical Engineers, Part L: Journal of Materials: Design and Applications, 237(3), 714–723, 2023. https://doi.org/10.1177/14644207221123142.

Seculi, F., Espinach, F.X., Julián, F., Delgado-Aguilar, M., Mutjé, P., Tarrés, Q., Evaluation of the strength of the interface for abaca fiber reinforced HDPE and BioPE composite materials, and its influence over tensile properties, Polymers, 14(24), 5412, 2022. https://doi.org/10.3390/polym14245412.

Seculi, F., Espinach, F.X., Julián, F., Delgado-Aguilar, M., Mutjé, P., Tarrés, Q., Comparative evaluation of the stiffness of abaca-fiber-reinforced bio-polyethylene and high density polyethylene composites, Polymers, 15(5), 1096, 2023a. https://doi.org/10.3390/polym15051096.

Seculi, F., Espinach, F.X., Julián, F., Delgado-Aguilar, M., Mutjé, P., Tarrés, Q., Evaluation of the interface strength in the abaca-fiber-reinforced bio-polyethylene composites, Polymers, 15(12), 2686, 2023b. https://doi.org/10.3390/polym15122686.

Seculi, F., Julián, F., Llorens, J., Espinach, F.X., Mutjé, P., Tarrés, Q., Methodologies to evaluate the micromechanics flexural strength properties of natural-fiber-reinforced composites: The case of abaca-fiber-reinforced bio polyethylene composites, Polymers, 15(14), 3137, 2023c. https://doi.org/10.3390/polym15143137.

Sinha, A.K., Bhattacharya, S., Narang, H.K., Abaca fibre reinforced polymer composites: A review, Journal of Materials Science, 56(7), 4569–4587, 2021. https://doi.org/10.1007/s10853-020-05572-9.

Vadivel, E., Venkatesh, R., Concentration of SiC and abaca fiber processing on functional properties of polypropylene hybrid composites, Journal of Mechanical Science and Technology, 39(11), 6713–6718, 2025. https://doi.org/10.1007/s12206-025-1018-3.

Valverde, J.C., Araya, M., Arias-Aguilar, D., Masís, C., Muñoz, F., Evaluation of the optimal uses of five genotypes of Musa textilis fiber grown in the tropical region, Polymers, 14(9), 1772, 2022. https://doi.org/10.3390/polym14091772.

Valášek, P., Müller, M., Šleger, V., Kolář, V., Hromasová, M., D'Amato, R., Ruggiero, A., Influence of alkali treatment on the microstructure and mechanical properties of coir and abaca fibers, Materials, 14(10), 2636, 2021. https://doi.org/10.3390/ma14102636.